The Journal of Experimental Biology 208, 799-808
Published by The Company of Biologists 2005
doi:10.1242/jeb.01435

Ankle plantar flexor force production is an important determinant of the preferred walk-to-run transition speed

Richard R. Neptune* and Kotaro Sasaki

Department of Mechanical Engineering, The University of Texas at Austin, Austin, TX 78712, USA

*Author for correspondence (e-mail: rneptune@mail.utexas.edu)

Accepted 13 December 2004

Summary

The mechanisms that govern the voluntary transition from walking to running as walking speed increases in human gait are not well understood. The objective of this study was to examine the hypothesis that plantar flexor muscle force production is greatly impaired at the preferred transition speed (PTS) due to intrinsic muscle properties and, thus, serves as a determinant for the walk-to-run transition. The plantar flexors have been shown to be important contributors to satisfying the mechanical energetic demands of walking and are the primary contributors to the observed ground reaction forces (GRFs) during the propulsion phase. Thus, if the plantar flexor force production begins to diminish near the PTS despite an increase in muscle activation, then a corresponding decrease in the GRFs during the propulsion phase would be expected. This expectation was supported. Both the peak anterior/posterior and vertical GRFs decreased during the propulsion phase at walking speeds near the PTS. A similar decrease was not observed during the braking phase. Further analysis using forward dynamics simulations of walking at increasing speeds and running at the PTS revealed that all lower extremity muscle forces increased with walking speed, except the ankle plantar flexors. Despite an increase in muscle activation with walking speed, the gastrocnemius muscle force decreased with increasing speed, and the soleus force decreased for walking speeds exceeding 80% PTS. These decreases in force production were attributed to the intrinsic force–length–velocity properties of muscle. In addition, the running simulation analysis revealed that the plantar flexor forces nearly doubled for similar activation levels when the gait switched to a run at the PTS due to improved contractile conditions. These results suggest the plantar flexors may serve as an important determinant for the walk-to-run transition and highlight the important role intrinsic muscle properties play in determining the specific neuromotor strategies used in human locomotion.

Key words: gait, intrinsic muscle properties, modeling and simulation.

Introduction

The mechanisms that govern the voluntary transition in human gait from walking to running as walking speed increases have received much attention from both experimental and theoretical perspectives. The preferred transition speed (PTS) occurs near 2 m s^{-1} (e.g. Hreljac, 1993a; Prilutsky and Gregor, 2001; Thorstensson and Roberthson, 1987), with many metabolic and biomechanical factors having been put forth as possible mechanisms for triggering the transition (e.g. Hanna et al., 2000; Raynor et al., 2002). Studies examining the relationships between metabolic cost and the PTS have provided conflicting results. A few studies have suggested that the walk-to-run transition is closely linked to the minimization of metabolic cost (Hanna et al., 2000; Mercier et al., 1994; Minetti and Alexander, 1997) while others have determined that the metabolically optimal speed is significantly greater than the PTS regardless of age, gender or gradient (Brisswalter and Mottet, 1996; Hreljac, 1993b; Minetti et al., 1994; Tseh et al., 2002). Previous studies have also proposed purely mechanical mechanisms based on inverted pendulum models, including analyses of the dimensionless Froude number (e.g. Alexander, 1989). The PTS occurs at a Froude number of approximately 0.5, even in reduced gravity environments (Kram et al., 1997), although it is unclear why the transition occurs at that particular dimensionless speed.

Examining various biomechanical factors, Hreljac (1995a) proposed that critical levels of high ankle dorsiflexion angular velocity occur during swing that cause the dorsiflexors to operate near their maximum capacity at the PTS. While he suggested that the transition from walking to running occurs to prevent dorsiflexor overexertion during the swing phase, his data would also be consistent with preventing overexertion of the plantar flexors. His data shows that the highest ankle angular velocity actually occurs in plantar flexion during the push-off phase, which is the region of highest ankle plantar flexor activity and muscle power output during walking (e.g. Neptune et al., 2001). Because of the increased plantar flexion angle and velocity with walking speed, the contractile state of the plantar flexors may be greatly impaired due to intrinsic

muscle properties (i.e. the muscle force–length–velocity relationships) as walking speed approaches the PTS. The ankle plantar flexor muscles have been shown to be important contributors to support, forward progression and swing initiation during normal walking (Neptune et al., 2004a; Zajac et al., 2003) and various clinical studies have suggested that the plantar flexors are a limiting factor in achieving higher walking speeds (e.g. Mueller et al., 1995; Nadeau et al., 1999; Olney et al., 1994).

We hypothesize that plantar flexor muscle force production is greatly impaired at walking speeds near the PTS due to poor contractile conditions and, therefore, necessitates a change in gait mode. Previous analyses of the walk–run transition have suggested that for a variable to be considered as a determinant of the transition, the variable should be near its maximum value as walking speed approaches the PTS, and then decrease to an acceptable level when gait is changed to a run (e.g. Hreljac, 1993b, 1995a). However, with our hypothesis we predict that the plantar flexor force would actually increase after the transition to a run due to an improved contractile state (assuming the muscle activation remains similar), which would make running at the PTS more effective in satisfying the increasing energetic demands of faster movement speeds.

To test this hypothesis, the anterior/posterior and vertical ground reaction forces (GRFs) across a wide range of walking speeds, including the PTS, were analyzed. Previous studies have shown that the peak GRFs increase with walking speed (e.g. Hreljac, 1993b; Nilsson and Thorstensson, 1989) and recent modeling and simulation studies have shown that the ankle plantar flexors are the primary contributors to the peak anterior/posterior and vertical GRFs during the propulsion phase in late stance (Anderson and Pandy, 2003; Neptune et al., 2004a). Thus, if the plantar flexor force production decreases near the PTS as hypothesized, then the peak GRFs during the propulsion phase at the PTS would also be expected to decrease. The GRF data presented in Nilsson and Thorstensson (1989) across a wide range of walking speeds provides evidence that such a phenomenon may occur; however, the data in that study were not analyzed relative to the PTS of their subjects. In addition, forward dynamics simulations actuated by individual musculotendon actuators were generated that emulated human subjects walking at increasing speeds and running at the PTS to examine the contractile state and force production of the ankle plantar flexors. The combination of the experimental and simulation analyses would provide important insight into the influence of the ankle plantar flexors on the walk-to-run PTS.

Materials and methods

Ten subjects (five male, five female; age 29.6±6.1 years; height 169.7±10.9 cm; mass 65.6±10.7 kg) walked at speeds of 40, 60, 80, 100 and 120% of their PTS and ran at 100% PTS on a split-belt instrumented treadmill (Tecmachine, Andrezieux Boutheon, France) while muscle EMG, three-dimensional GRFs and body segment motion data from the right leg were collected using a motion capture system (Motion Analysis Corp., Santa Rosa, CA, USA) at 2000, 480 and 120 Hz, respectively, for 15 s at each randomly assigned speed. To identify each subject's PTS, a stepped protocol was used. Starting at 0.6 m s^{-1}, each subject walked on the treadmill while its speed was systematically increased in increments of 0.1 m s^{-1} every 30 s and the speed at which the subject preferred to run rather than walk during the entire 30 s duration was deemed their PTS. The process was repeated three times and the average value was determined. Prior to the data collection, all subjects provided informed consent according to the rules and regulations of the Cleveland Clinic Foundation and The University of Texas at Austin.

The EMG data were collected using disposable surface bipolar electrodes (Noraxon, Scottsdale, AZ; 1 cm diameter, 2 cm inter-electrode distance) from the right soleus (SOL), medial gastrocnemius (GAS), tibialis anterior (TA), gluteus maximus (GMAX), vasti medialis (VAS), biceps femoris long-head (BF) and rectus femoris (RF), which were used to assist in the generation of simulations of walking and running (see *Forward dynamics simulations* below). Electrode placements were based on the guidelines provided by Perotto (1994) and all signals were checked for clarity and strength of signal during isolated isometric movements. The data were band-pass filtered (20–400 Hz), fully rectified and then low-pass filtered at 10 Hz using a fourth order zero-lag digital Butterworth filter. The EMG linear envelope was then normalized to its maximum value during walking at 120% of each subject's PTS. The body segment motion data were measured using a modified Helen Hayes marker set and corresponding joint angles were determined. The GRF and motion data were filtered with a 4th order zero-lag Butterworth filter with cut-off frequencies of 20 and 6 Hz, respectively and joint angular velocities were calculated using a finite-difference approximation. The stance phase was divided into the braking and propulsion phase as determined from the anterior/posterior GRF (braking phase when the anterior/posterior force is negative, ~0–30% gait cycle; propulsion phase when the anterior/posterior force is positive, ~30–60% gait cycle). The peak anterior/posterior and vertical GRFs during each phase were determined at each speed. Data were averaged across 10 consecutive walking cycles within each subject at each speed, and then across subjects to obtain a group average.

A repeated-measures analysis of variance was used to assess whether the peak anterior/posterior and vertical GRFs within the braking and propulsion phases were significantly affected by walking speed ($P<0.05$). In addition, the peak SOL, GAS and TA EMG magnitudes over the gait cycle were also examined. When significant effects were detected within a quantity, pairwise comparisons with a Bonferroni adjustment to account for the multiple comparisons were performed to identify which speeds were significantly different.

Forward dynamics simulations

Forward dynamics simulations of walking at 60, 80, 100 and 120% PTS and running at 100% PTS were generated using a

previously described musculoskeletal modeling and dynamic optimization framework (e.g. Neptune et al., 2004b) to analyze the contractile state and force production of the major lower extremity muscle groups. The sagittal-plane biped musculoskeletal model was developed using SIMM (MusculoGraphics Inc., Evanston, IL, USA) and the equations of motion of the model were generated using SD/FAST (PTC, Needham, MA, USA). The equations of motion were then incorporated into simulation code generated by the Dynamics Pipeline (MusculoGraphics Inc., Evanston, IL, USA). Details of the musculoskeletal model and dynamic optimization that were used to produce the forward dynamics simulations emulating the experimentally collected kinesiological data of walking and running are provided below.

Musculoskeletal model

The musculoskeletal model included a trunk (head, arms and torso combined as one segment) and right and left legs (each leg containing a femur, tibia, patella and foot) (Fig. 1). The model yielded nine degrees-of-freedom including hip, knee and ankle flexion/extension for both legs, and trunk horizontal and vertical translation and anterior/posterior tilting. The knee flexion angle was used to prescribe two translational degrees-of-freedom of the knee joint (Yamaguchi and Zajac, 1989) and the position and orientation of the patella relative to the femur (Delp et al., 1990). Thirty visco-elastic elements were attached to the bottom of each foot segment to model the contact between the foot and ground. Details of the model and parameter values are provided in Neptune et al. (2000). The same foot–ground contact model parameters were used for both the walking and running simulations.

Fifteen Hill-type musculotendon actuators including tendon compliance (Fig. 2) per leg were used to actuate the model, which were combined into nine muscle groups based on anatomical classification with muscles within each group receiving the same excitation pattern. The nine muscle groups were defined as IL (iliacus, psoas), GMAX (gluteus maximus, adductor magnus), VAS (three-component vastus), HAM (medial hamstrings, biceps femoris long head), SOL (soleus), BFsh (biceps femoris short head), GAS (medial and lateral gastrocnemius), RF (rectus femoris) and TA (tibialis anterior). The muscle force generating capacity was governed by normalized force–length and force–velocity relationships (Fig. 3), and a normalized non-linear tendon force–strain relationship to describe tendon force (Delp and Loan, 1995; Zajac, 1989). All musculotendon parameters were based on the work of Delp et al. (1990). The muscle activation–deactivation dynamics was represented with a first-order differential equation (Raasch et al., 1997) with activation and deactivation time constants of 5 and 10 ms, respectively. Passive joint torques representing ligaments and other connective tissues were used to limit the joint range of motion at extreme joint angles (Davy and Audu, 1987).

Dynamic optimization

The experimentally collected EMG linear envelopes were used to define the muscle excitation patterns in the simulations and dynamic optimization was used to modify the excitation patterns to produce well coordinated walking and running motions. For those muscles from which EMG were not measured (IL, BFsh), a block excitation pattern was used with excitation timing similar to Perry (1992). A simulated annealing optimization algorithm (Goffe et al., 1994) was used to fine-tune the excitation patterns by adjusting three parameters per muscle corresponding to the excitation pattern onset, duration and magnitude until the difference between the experimental and simulated kinematic and ground reaction force data was minimized (e.g. Neptune et al., 2001). Constraints were placed on the excitation timing in the optimization to closely replicate the EMG timing (i.e. EMG nominal values ± 10% gait cycle) to assure that the muscles were active at the appropriate region in the gait cycle. The muscle excitation patterns were assumed symmetrical between the left and right legs. The specific tracking quantities used in the objective function included trunk translation and tilting, all

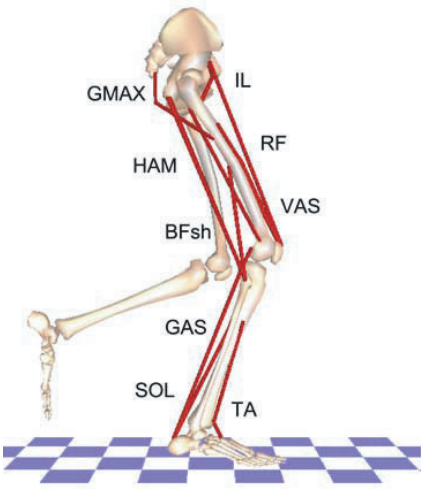

Fig. 1. Bipedal musculoskeletal model including the nine muscle groups per leg used to simulate walking and running.

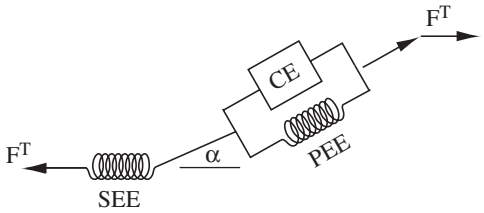

Fig. 2. Schematic of the musculotendon actuator used in the model. The properties of the musculotendon force generation (F^T) were represented by an active contractile element (CE) in parallel with a passive elastic element (PEE). The muscle fiber was placed in series with tendon (SEE), which was represented by a non-linear elastic element. The pennation angle (α) denotes the angle between the muscle fibers and the tendon. All musculotendon parameters, including the origin and insertion of each muscle, pennation angle, tendon slack length, resting fiber length and maximum isometric force were based on Delp et al. (1990).

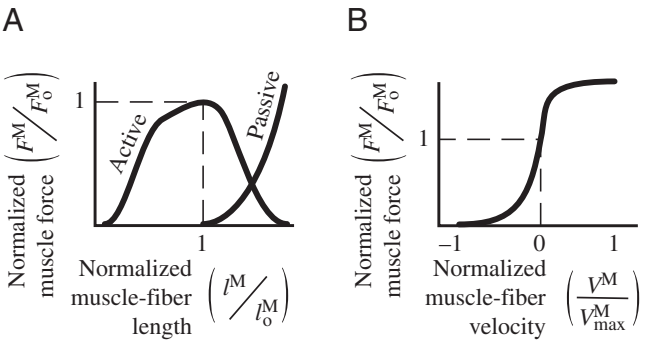

Fig. 3. Intrinsic muscle properties: (A) normalized force–length and (B) force–velocity relationships (Delp and Loan, 1995; Zajac, 1989). With deviations from the muscle fiber's optimal length and increasing rates of shortening, the ability of a muscle to produce force decreases. Note, negative velocity values indicate muscle shortening.

joint angles and the anterior/posterior and vertical GRFs. The tracking data collected from the subjects' right side were shifted 50% of the gait cycle to provide data for the left side. A simulation of 1.5 gait cycles was generated, with the objective function being evaluated during the final full gait cycle to assure the initial start-up transients had decayed.

Muscle contractile state

From the walking and running simulations, individual muscle fiber lengths and velocities over the gait cycle were determined from the model and normalized to the optimal fiber length and maximum contraction velocity of the muscle, respectively. The optimal fiber lengths were based on the work of Delp et al. (1990) and each muscle's maximum shortening velocity was estimated as ten times the muscle fiber optimal length per second (Zajac, 1989). In addition, individual musculotendon forces and activation levels were quantified.

Results

Experimental analysis

The group average preferred transition speed (PTS) was 1.96±0.17 m s^{-1} (male 1.94±0.20 m s^{-1}; female 1.98±0.17 m s^{-1}). The EMG magnitudes and braking phase GRFs systematically increased at all walking speeds. The peak SOL and GAS magnitude occurred during the propulsion phase (~40% gait cycle), and the peak TA activity occurred in late swing (~90% gait cycle) (Fig. 4). The peak SOL, GAS and TA EMG magnitude significantly increased over the whole range of walking speeds studied (Fig. 4) (P<0.05). The only exceptions were that no significant differences in peak magnitude at the two slowest speeds (40% and 60% PTS) were found for SOL and GAS. The peak anterior/posterior and vertical GRFs during the braking phase also systematically increased with walking speed (Fig. 5, Table 1), with all values being significantly different from the previous speed except for the anterior/posterior braking force at 120% PTS.

By contrast, during the propulsion phase the GRFs decreased at and beyond the PTS. The trend for the peak

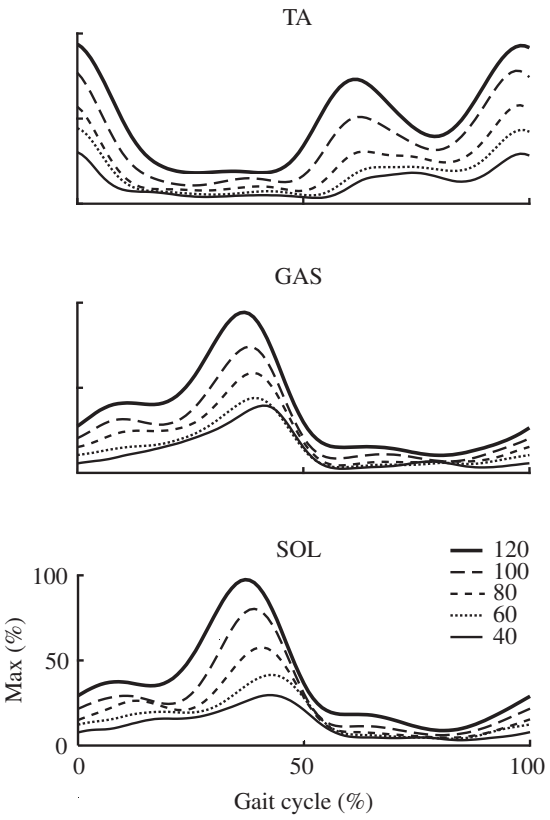

Fig. 4. Normalized experimental soleus (SOL), medial gastrocnemius (GAS) and tibialis anterior (TA) muscle EMG as walking speed increased from 40 to 120% PTS. The EMG magnitude of all muscles continued to increase beyond the PTS.

vertical GRF was to increase with walking speed up to 80% PTS, and then to decrease at 120% PTS (P<0.05) (Fig. 5, Table 1). Similarly, the peak anterior/posterior GRF systematically increased with walking speed up to the PTS, with all values being significantly higher than the previous value (P<0.05). By contrast, between 100% and 120% PTS no significant difference in magnitude was observed (Fig. 5, Table 1) (P<0.05). This finding was consistent among subjects as the peak anterior/posterior and vertical GRFs during the propulsion phase were lower at 120% PTS compared with 100% PTS in 8 out of 10 subjects.

Simulation analysis

The dynamic optimization produced walking and running simulations that emulated the human subject tracking data to within ± 2 S.D. (e.g. Fig. 6). The simulation data showed that muscle activation and force both systematically increased with walking speed in all muscles except for the plantar flexors. Although both GAS and SOL activation increased with walking speed (Fig. 7A), as did the other muscles, the force produced by GAS decreased with walking speed and SOL force began to decrease after walking speed exceeded 80% PTS (Fig. 7A). Examination of the contractile state of the plantar flexors near peak muscle activation and force production as walking speed increased revealed that the SOL

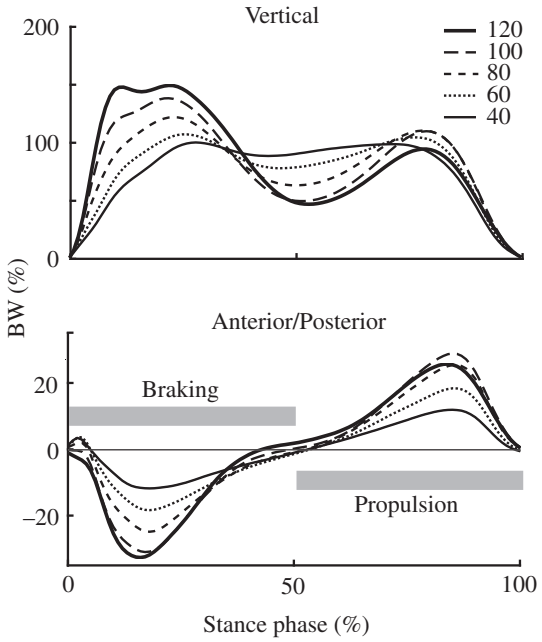

Fig. 5. Experimental anterior/posterior and vertical ground reaction forces as walking speed increased from 40 to 120% PTS. The braking and propulsion phases are indicated with grey horizontal bars during 100% PTS walking.

Table 1. *Peak ground reaction forces*

	Ground reaction forces		Walking speed
	Anterior/posterior	Vertical	(% PTS)
Braking phase	–0.12±0.01	1.03±0.03	40
	–0.18†±0.00	1.10†±0.03	60
	–0.25†±0.00	1.25†±0.06	80
	–0.31†±0.01	1.43†±0.20	100
	–0.34±0.01	1.61†±0.25	120
Propulsion phase	0.13±0.02	1.02±0.02	40
	0.19†±0.04	1.07†±0.03	60
	0.26†±0.04	1.13±0.02	80
	0.30†±0.06	1.12±0.08	100
	0.27±0.09	0.97†±0.12	120

Peak experimental anterior/posterior and vertical ground reaction forces (GRF) (mean ± 1 S.D.) as walking speed increased from 40 to 120% PTS. During the braking phase, the peak anterior/posterior and vertical GRFs continued to increase beyond the PTS. However, during the propulsive phase, the vertical GRF increases up to 80% PTS, and then begins to decrease at the PTS, with the value at 120% PTS being significantly lower. Similarly, the anterior/posterior GRF increases up to the PTS and then the trend abruptly changes after the PTS [†indicates the value is significantly different than the value at the previous speed (P<0.05)]. Note, the GRF values are normalized to body weight.

and GAS normalized fiber lengths systematically shortened and approached 0.6 and 0.7, respectively (Fig. 7B), and both normalized shortening fiber velocities systematically increased and approached –0.25 (Fig. 7B), which were adverse contractile conditions for producing muscle force (Fig. 3).

By contrast, all other muscle groups produced greater force as walking speed increased (e.g. TA; Fig. 7A), which was due to an improved contractile state compared with the plantar flexors. For example, the TA normalized fiber length and velocity at peak activation in swing at the fastest walking speed was 0.8 and –0.1, respectively (Fig. 7B). The simulation data of the same subjects running at the PTS revealed that the contractile state of the plantar flexors was greatly improved after the transition from walking to running, which produced greater muscle force for similar levels of activation. SOL produced 90% more peak force and GAS 86% more peak force during their active region even though their activation levels in the simulations only increased by 10% and 27%, respectively (Fig. 8; SOL and GAS).

Discussion

The main objective of this study was to test the hypothesis that plantar flexor muscle force production is greatly impaired near the PTS due to poor contractile conditions and, thus, may serve as a determinant for the walk-to-run transition. The plantar flexors have been shown to be important contributors to support, forward progression and swing initiation (e.g. Neptune et al., 2001; Zajac et al., 2003) and to be the primary contributors to the observed anterior/posterior and vertical

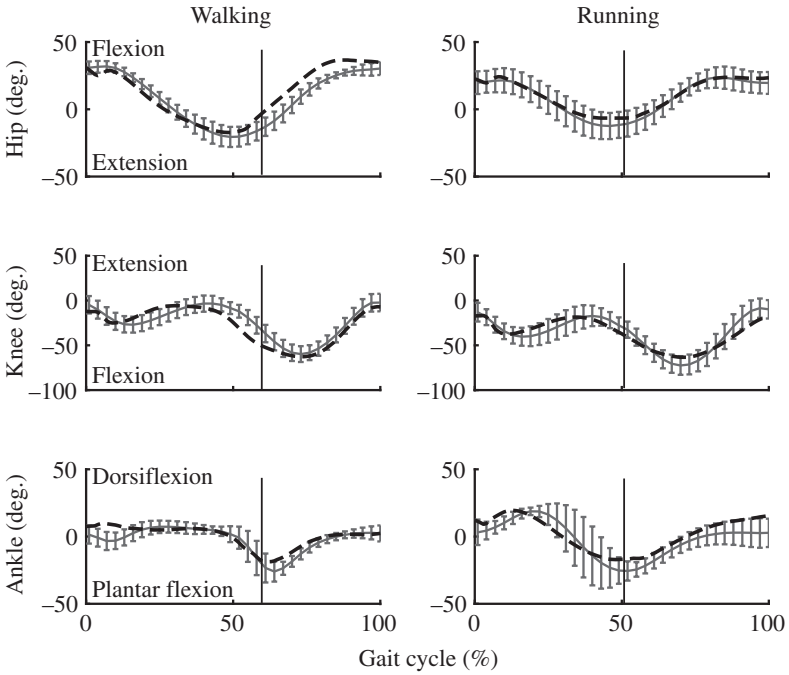

Fig. 6. Simulation tracking over the entire gait cycle of the hip, knee and ankle joint angles during walking and running at 100% PTS. The vertical lines indicate toe-off.

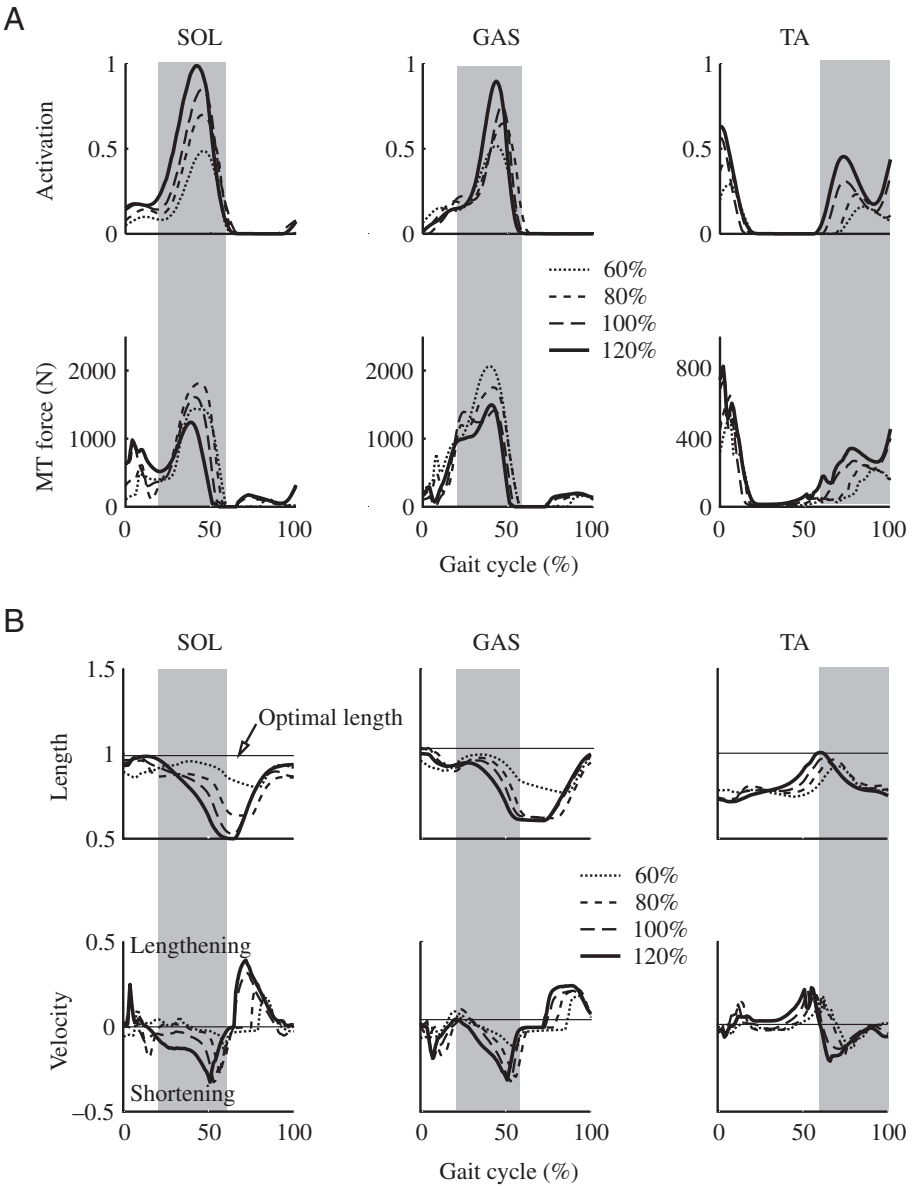

Fig. 7. Simulation results of walking as walking speed increases from 60 to 120% PTS for the soleus (SOL), medial gastrocnemius (GAS) and tibialis anterior (TA). (A) Muscle activation as a percent of maximum (Activation) and musculotendon force (MT force), and (B) normalized muscle fiber length and velocity. The fiber length was normalized to its optimal length and the velocity was normalized to its maximum contraction velocity, which was estimated as ten times the muscle fiber resting length per second (Zajac, 1989). Negative velocity values indicate muscle shortening. The gray filled regions indicate general area of muscle activity.

GRFs during the propulsion phase (Anderson and Pandy, 2003; Neptune et al., 2004a). Therefore, if the plantar flexor force production should begin to decrease near the PTS as hypothesized, then a corresponding decrease in the GRFs during the propulsion phase would be expected.

The experimental and simulation data supported these expectations. The peak propulsion-phase vertical GRF began to decrease at the PTS and the peak anterior/posterior force decreased slightly above the PTS (Fig. 5, Table 1). By contrast, the anterior/posterior and vertical GRFs during the braking phase increased over the whole range of speeds studied. These results are consistent with Nilsson and Thorstensson (1989) who performed a comprehensive GRF analysis across a wide range of walking speeds during overground walking. They found that the peak vertical and anterior/posterior GRFs during the braking phase increased with walking speed from 1.0 to 3.0 m s^{-1}, but the peak vertical and anterior/posterior GRFs during the propulsion phase began to decrease near 2.0 to 2.5 m s^{-1}, respectively, and continued to decrease up to 3.0 m s^{-1}. However, they did not examine the data relative to the PTS of the subjects in their study. The decrease in their GRFs began at slightly higher speeds than the present study. For example, the decrease in the peak vertical GRF occurred at a walking speed of 2.5 m s^{-1}, compared with 2.0 m s^{-1} for the subjects in the present study. The difference between studies could be related to subject training (Beaupied et al., 2003) or walking on a treadmill versus overground. We chose to analyze treadmill data because of the methodological advantage of being able to precisely control walking speed and collect a large number of consecutive step cycles to establish a steady-state walking pattern.

Li and Hamill (2002) also observed a decrease in the peak vertical GRF during the propulsion phase in the step preceding the walk-to-run transition during accelerated treadmill walking. Although they did not measure the anterior/posterior GRF due to treadmill limitations, they speculated that the decrease in the vertical GRF was a reconfiguration of the resultant GRF, and that the magnitude of the resultant force remains constant. However, our results showed that the peak anterior/posterior GRF also decreased. Li and Hamill (2002) also suggested that the decrease in the peak propulsive vertical GRF is an active or intentional behavior in anticipation of the gait transition, which would not occur if walking speed is increased and a transition is not intended. However, the results of the present study and those of Nilsson and Thorstensson (1989), which show a decrease in the steady-state GRFs when a transition is not intended, suggest that the decrease is not an active or intentional behavior, but may be the result of intrinsic muscle properties influencing muscle force production.

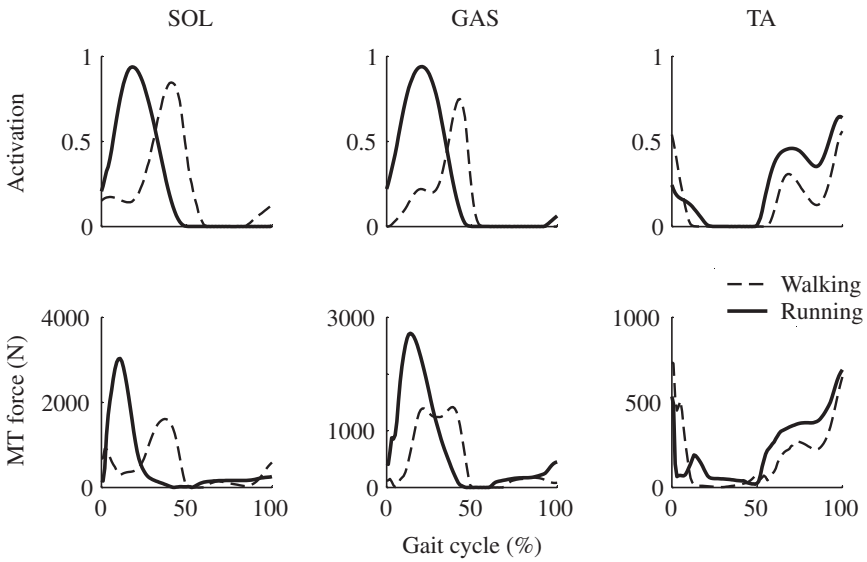

Fig. 8. Simulation muscle activation and force comparison between walking and running at 100% PTS.

The decrease in the vertical GRFs during the propulsion phase near the PTS and the decrease in the anterior/posterior GRF immediately after the PTS, despite an increase in ankle plantar flexor activity (Fig. 4), suggest that the ability of these muscles to produce force diminishes as walking speed approaches the PTS. Both the force–length and force–velocity relationships are intrinsic muscle properties that directly influence a muscle's ability to generate force, with active force diminishing with increasing speeds of contraction and as the fiber length deviates from its optimal (Fig. 3). Thus, if the plantar flexors are operating at increasingly adverse contractile lengths and velocities at walking speeds just prior to the PTS, the transition from a walk to a run at the PTS may place them at a better operating point on the force–length–velocity relationship since the ankle joint velocities at the PTS are lower in running than walking (e.g. Hreljac, 1995a). The transition would thus allow the plantar flexors to generate greater force for a given activation level to help satisfy the increasing energetic demands of faster movement speeds.

The simulation analysis supported this hypothesis. The simulation data showed that both activation and force production systematically increased with walking speed in all muscles except for the plantar flexors. The force produced by GAS decreased with walking speed and SOL force began to decrease after walking speed exceeded 80% PTS, despite an increase in GAS and SOL activation with walking speed (Fig. 7A). The contractile state of the plantar flexors near peak muscle activation and force revealed that the SOL and GAS normalized fiber lengths approached 0.6 and 0.7, respectively (Fig. 7B), and both normalized fiber velocities approached –0.25 (Fig. 7B). These velocity values would appear to be conservative estimates as the combined ankle and knee joint angular velocities during the propulsion phase near the PTS were lower in the simulation than the experimental data (Table 2). Thus the capacity of the plantar flexors to produce muscle force as walking speed approached the PTS was greatly impaired (Fig. 3).

By contrast, all other muscle groups produced higher force as walking speed increased. For example, TA has an optimal fiber length over two and three times the length of GAS and SOL, respectively (Delp et al., 1990), which provides a more favorable force-generating contractile state compared with the plantar flexors as walking speed increased (Fig. 7A). The TA normalized fiber length and velocity at peak activation in swing was 0.8 and –0.1, respectively (Fig. 7B). Hreljac (1995a) proposed that the dorsiflexor muscles perform at or near their maximum capacity at the PTS and may be susceptible to overexertion, and therefore serve as a determinant for the walk-to-run transition. However, our simulation results indicate that not only is the force–length–velocity state of TA much more favorable than the plantar flexors for producing force, but TA is activated far below its maximum. At 120% PTS, peak TA activation was only 60% of maximum (Fig. 7A), as opposed to the near 100% activation of the plantar flexors (Fig. 7A). The differences in levels of muscle activation are consistent with each muscle's contribution to the mechanical energetics of walking; TA is primarily responsible for providing toe clearance during early swing, while the plantar flexors are the primary contributors to body support, forward progression and swing initiation in late stance (Neptune et al., 2001; Zajac et

Table 2. *Peak joint angular velocities*

	Subjects	Simulation	Walking speed (% PTS)
Ankle	–5.66±0.78	–2.66	60
	–6.47±0.81	–3.44	80
	–6.55±0.77	–5.06	100
	–6.51±0.78	–4.47	120
Knee	–5.24±0.40	–6.25	60
	–5.62±0.38	–6.29	80
	–6.23±0.44	–6.49	100
	–7.36±0.74	–6.08	120

Comparison of the experimental (mean ± 1 S.D.) and simulation peak ankle (plantar flexion) and knee (flexion) joint angular velocities during the propulsion phase as walking speed increased from 60 to 120% PTS. In both joints, the experimental velocities systematically increased with walking speed, except for the slight decrease in the ankle velocity at 120% PTS. At all speeds, the corresponding simulation ankle velocities were lower than the experimental data, while the knee velocities were slightly higher except at 120% PTS.

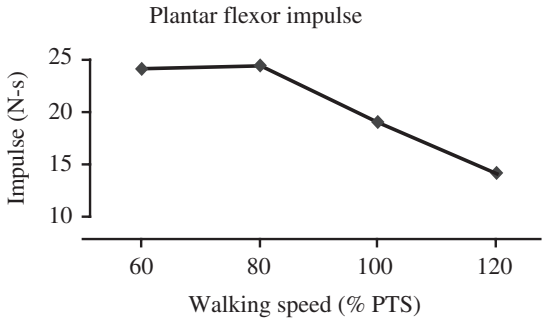

Fig. 9. Combined simulation plantar flexor muscle impulse from the soleus and medial gastrocnemius during the propulsion phase as walking speed increased from 60 to 120% PTS.

al., 2003). These results suggest that the plantar flexors, rather than the dorsiflexors, may be over-exerted at the PTS.

The overexertion of the plantar flexors near the PTS may also influence the walking mechanics. An important task requirement in walking is maintaining the necessary propulsive impulse over the gait cycle to conserve linear momentum and maintain a constant average walking speed. With our hypothesis that plantar flexor force production is impaired at higher walking speeds, we would predict that the impulse associated with the ankle plantar flexors would also decrease as walking speed approached the PTS. The planter flexor impulse is particularly important since the plantar flexors are the primary contributors to the observed anterior/posterior GRF during the propulsion phase (Anderson and Pandy, 2003; Neptune et al., 2004a). To test this prediction, we computed the total impulse generated by the plantar flexors during the propulsive phase in a *post hoc* analysis of the simulation data and found that the plantar flexor impulse remained relatively constant between walking speeds of 60 and 80% PTS, and then began to decrease dramatically as walking speed approached the PTS (Fig. 9). These results were consistent with Nilsson and Thorstensson (1989) who found that the total horizontal GRF propulsive impulse increased until 2.5 m s^{-1}, and then began to decrease at higher speeds. Thus, considering the important contributions of the plantar flexors to satisfying the task demands of walking (Neptune et al., 2001; Zajac et al., 2003), a decrease in the mechanical output of these important functional muscles as walking speed increases may necessitate a change in gait mode, and thus serve as a critical determinant for the walk-to-run transition.

With our plantar flexor hypothesis, we also predicted that the transition from walking to running would improve the contractile conditions of the plantar flexors, allowing them to produce greater muscle force for a given activation level and make running at the PTS more effective in satisfying the increasing energetic demands of faster movement speeds. The running simulation data at the PTS showed that the contractile state of the plantar flexors was indeed improved after the transition from walking to running. SOL produced 90% more peak force and GAS 86% more peak force during their active region even though their activation levels in the simulations only increased by 10% and 27%, respectively (Fig. 8; SOL and GAS). The increased muscle forces were attributed to improvements in the contractile state on both the force–length and force–velocity relationships. Thus, the transition from walking to running at the PTS provides a large increase in plantar flexor force production for a small increase in activation. By contrast, the TA force levels were similar in both walking and running (Fig. 8; TA). Further research is needed to assess whether the increase in force production during running allows the plantar flexors to perform the same functional tasks as in walking or if differences in the running mechanics causes a reorganization of how individual muscles work together in synergy to satisfy the task requirements. Further, running provides the advantage of increased elastic energy storage and return in the plantar flexor tendons (e.g. Hof et al., 2002; Kram, 2000), but it is unclear to what degree other muscle groups exploit similar energy efficient mechanisms.

The results of this study suggest that normalized intrinsic muscle properties (i.e. force–length–velocity relationships) play an important role in the determination of the specific neuromotor strategies used by the nervous system in human locomotion. Previous studies have shown little success in identifying correlations between various anthropometric measurements (e.g. body dimensions, inertial characteristics and strength) and the PTS (Getchell and Whitall, 1997; Hanna et al., 2000; Hreljac, 1995b; Thorstensson and Roberthson, 1987). Unlike individual anthropometric measurements, normalized intrinsic muscle properties are relatively homogeneous across humans (e.g. Zajac, 1989), and therefore would provide a consistent transition mechanism regardless of variations in anthropometrics, age and gender (e.g. Hanna et al., 2000; Hreljac, 1993b; Tseh et al., 2002). The state of the plantar flexor's functional capacity in relation to the force–length and force–velocity relationships could be conveyed by integration of the proprioceptive feedback, which has been previously proposed as an important feedback mechanism influencing the walk-to-run transition (Hreljac, 1995a; Raynor et al., 2002; Thorstensson and Roberthson, 1987). Hreljac (1995a) has suggested that proprioceptive feedback is used to indicate local discomfort and fatigue in the ankle dorsiflexors, and Raynor et al. (2002) suggested that feedback is necessary to determine the potential use of stored elastic energy in tendons. In addition, the state of the plantar flexors on the force–length–velocity relationships would be conveyed through the integration of sensory information from the muscle spindles (length and velocity of muscle stretch) and Golgi tendon organs (muscle tension) to indicate a change in gait mode is necessary. Using such sensory feedback as a determinant for the walk–run transition is consistent with the idea that the transition between gait modes is most likely initiated by some step-by-step criterion (Saibene and Minetti, 2003).

A potential confounding factor is that the Hill-type muscle model used in our simulations did not account for all of the relationships between force, length, velocity and activation (for review see Huijing, 1998) and the time-dependence of muscle

force production (for review see Herzog, 1998). However, both the experimental and simulation data support the hypothesis that ankle plantar flexor force output plateaus or diminishes as walking speed approaches the PTS due to intrinsic muscle properties, primarily the force–length and force–velocity relationships. As walking speed increases, the plantar flexion angle and velocity increases in a monotonic fashion (e.g. Lelas et al., 2003; Winter, 1991), which causes the plantar flexors to operate at shorter lengths and higher velocities during the propulsion phase (Fig. 7) when critical levels of plantar flexor force production are required to satisfy the task demands. Thus, given the need for the plantar flexors to produce a given level of force to produce the observed kinematics, we believe muscle activation would change to accommodate the unmodeled complex intrinsic muscle properties (e.g. force deficit or depression following active shortening, Herzog, 1998; Huijing, 1998) just as activation changes to accommodate less force production due to shorter fiber lengths and faster fiber shortening velocities (Figs 4 and 8). The overall trend of the plantar flexor contractile state towards becoming increasingly adverse for producing muscle force as walking speed approaches the PTS would, therefore, remain.

Although this study does not exclude the many proposed kinetic, kinematic and energetic determinants for the walk-to-run transition (e.g. Hanna et al., 2000; Raynor et al., 2002), the analysis of the GRFs and contractile state of the lower extremity muscles do support the proposed hypothesis that the ankle plantar flexors are operating under adverse contractile conditions near the PTS. Thus, a change in gait mode would be necessary to effectively move at higher speeds. These results highlight the important role intrinsic muscle properties play in determining the specific neuromotor strategies used in human locomotion. Future work will be directed at assessing if similar mechanisms hold for the run-to-walk transition.

The authors are grateful to The Whitaker Foundation for financial support of this work and Julie Perry, Brian Davis and Ton van den Bogert for help with the data collection. In addition, the authors would like to acknowledge the insightful comments on a previous version of the manuscript from Steve Kautz and Felix Zajac.

References

Alexander, R. M. (1989). Optimization and gaits in the locomotion of vertebrates. *Physiol. Rev.* **69**, 1199-1227.

Anderson, F. C. and Pandy, M. G. (2003). Individual muscle contributions to support in normal walking. *Gait Posture* **17**, 159-169.

Beaupied, H., Multon, F. and Delamarche, P. (2003). Does training have consequences for the walk–run transition speed? *Hum. Mov. Sci.* **22**, 1-12.

Brisswalter, J. and Mottet, D. (1996). Energy cost and stride duration variability at preferred transition gait speed between walking and running. *Can. J. Appl. Physiol.* **21**, 471-480.

Davy, D. T. and Audu, M. L. (1987). A dynamic optimization technique for predicting muscle forces in the swing phase of gait. *J. Biomech.* **20**, 187-201.

Delp, S. L. and Loan, J. P. (1995). A graphics-based software system to develop and analyze models of musculoskeletal structures. *Comput. Biol. Med.* **25**, 21-34.

Delp, S. L., Loan, J. P., Hoy, M. G., Zajac, F. E., Topp, E. L. and Rosen, J. M. (1990). An interactive graphics-based model of the lower extremity to study orthopaedic surgical procedures. *IEEE Trans. Biomed. Eng.* **37**, 757-767.

Getchell, N. and Whitall, J. (1997). Transitions in gait as a function of physical parameters (abstract). *J. Sport Exercise Psychol.* **19**, S55.

Goffe, W. L., Ferrier, G. D. and Rogers, J. (1994). Global optimization of statistical functions with simulated annealing. *J. Econometrics* **60**, 65-99.

Hanna, A., Abernethy, B., Neal, R. J. and Burgess-Limerick, R. (2000). Triggers for the transition between human walking and running. In *Energetics of Human Activity* (ed. W. A. Sparro), pp. 124-164. Chicago: Human Kinetics.

Herzog, W. (1998). History dependence of force production in skeletal muscle: a proposal for mechanisms. *J. Electromyogr. Kinesiol.* **8**, 111-117.

Hof, A. L., Van Zandwijk, J. P. and Bobbert, M. F. (2002). Mechanics of human triceps surae muscle in walking, running and jumping. *Acta Physiol. Scand.* **174**, 17-30.

Hreljac, A. (1993a). Preferred and energetically optimal gait transition speeds in human locomotion. *Med. Sci. Sports Exerc.* **25**, 1158-1162.

Hreljac, A. (1993b). Determinants of the gait transition speed during human locomotion: kinetic factors. *Gait Posture* **1**, 217-223.

Hreljac, A. (1995a). Determinants of the gait transition speed during human locomotion: kinematic factors. *J. Biomech.* **28**, 669-677.

Hreljac, A. (1995b). Effects of physical characteristics on the gait transition speed during human locomotion. *Hum. Mov. Sci.* **14**, 205-216.

Huijing, P. A. (1998). Muscle, the motor of movement: properties in function, experiment and modelling. *J. Electromyogr. Kinesiol.* **8**, 61-77.

Kram, R. (2000). Muscular force or work: what determines the metabolic energy cost of running? *Exerc. Sport Sci. Rev.* **28**, 138-143.

Kram, R., Domingo, A. and Ferris, D. P. (1997). Effect of reduced gravity on the preferred walk–run transition speed. *J. Exp. Biol.* **200**, 821-826.

Lelas, J. L., Merriman, G. J., Riley, P. O. and Kerrigan, D. C. (2003). Predicting peak kinematic and kinetic parameters from gait speed. *Gait Posture* **17**, 106-112.

Li, L. and Hamill, J. (2002). Characteristics of the vertical ground reaction force component prior to gait transition. *Res. Q. Exerc. Sport* **73**, 229-237.

Mercier, J., Le Gallais, D., Durand, M., Goudal, C., Micallef, J. P. and Prefaut, C. (1994). Energy expenditure and cardiorespiratory responses at the transition between walking and running. *Eur. J. Appl. Physiol. Occup. Physiol.* **69**, 525-529.

Minetti, A. E. and Alexander, R. M. (1997). A theory of metabolic costs for bipedal gaits. *J. Theor. Biol.* **186**, 467-476.

Minetti, A. E., Ardigo, L. P. and Saibene, F. (1994). The transition between walking and running in humans: metabolic and mechanical aspects at different gradients. *Acta Physiol. Scand.* **150**, 315-323.

Mueller, M. J., Minor, S. D., Schaaf, J. A., Strube, M. J. and Sahrmann, S. A. (1995). Relationship of plantar-flexor peak torque and dorsiflexion range of motion to kinetic variables during walking. *Phys. Ther.* **75**, 684-693.

Nadeau, S., Gravel, D., Arsenault, A. B. and Bourbonnais, D. (1999). Plantarflexor weakness as a limiting factor of gait speed in stroke subjects and the compensating role of hip flexors. *Clin. Biomech.* **14**, 125-135.

Neptune, R. R., Wright, I. C. and van den Bogert, A. J. (2000). A method for numerical simulation of single limb ground contact events: application to heel-toe running. *Comp. Meth. Biomech. Biomed. Eng.* **3**, 321-334.

Neptune, R. R., Kautz, S. A. and Zajac, F. E. (2001). Contributions of the individual ankle plantar flexors to support, forward progression and swing initiation during walking. *J. Biomech.* **34**, 1387-1398.

Neptune, R. R., Zajac, F. E. and Kautz, S. A. (2004a). Muscle force redistributes segmental power for body progression during walking. *Gait Posture* **19**, 194-205.

Neptune, R. R., Zajac, F. E. and Kautz, S. A. (2004b). Muscle mechanical work requirements during normal walking: the energetic cost of raising the body's center-of-mass is significant. *J. Biomech.* **37**, 817-825.

Nilsson, J. and Thorstensson, A. (1989). Ground reaction forces at different speeds of human walking and running. *Acta Physiol. Scand.* **136**, 217-227.

Olney, S. J., Griffin, M. P. and McBride, I. K. (1994). Temporal, kinematic, and kinetic variables related to gait speed in subjects with hemiplegia – a regression approach. *Phys. Ther.* **74**, 872-885.

Perotto, A. (1994). Anatomical guide for the electromyographer: the limbs and trunk. Springfield, IL: Charles C Thomas Publisher.

Perry, J. (1992). Gait analysis: normal and pathological function. Thorofare, NJ: Slack Inc.

Prilutsky, B. I. and Gregor, R. J. (2001). Swing- and support-related muscle

actions differentially trigger human walk–run and run-walk transitions. *J. Exp. Biol.* **204**, 2277-2287.

Raasch, C. C., Zajac, F. E., Ma, B. and Levine, W. S. (1997). Muscle coordination of maximum-speed pedaling. *J. Biomech.* **30**, 595-602.

Raynor, A. J., Yi, C. J., Abernethy, B. and Jong, Q. J. (2002). Are transitions in human gait determined by mechanical, kinetic or energetic factors? *Hum. Mov. Sci.* **21**, 785-805.

Saibene, F. and Minetti, A. E. (2003). Biomechanical and physiological aspects of legged locomotion in humans. *Eur. J. Appl. Physiol.* **88**, 297-316.

Thorstensson, A. and Roberthson, H. (1987). Adaptations to changing speed in human locomotion: speed of transition between walking and running. *Acta Physiol. Scand.* **131**, 211-214.

Tseh, W., Bennett, J., Caputo, J. L. and Morgan, D. W. (2002). Comparison between preferred and energetically optimal transition speeds in adolescents. *Eur. J. Appl. Physiol.* **88**, 117-121.

Winter, D. A. (1991). The biomechanics and motor control of human gait: normal, elderly and pathological. Waterloo, Ont.: Waterloo Biomechanics.

Yamaguchi, G. T. and Zajac, F. E. (1989). A planar model of the knee joint to characterize the knee extensor mechanism. *J. Biomech.* **22**, 1-10.

Zajac, F. E. (1989). Muscle and tendon: properties, models, scaling, and application to biomechanics and motor control. *Crit. Rev. Biomed. Eng.* **17**, 359-411.

Zajac, F. E., Neptune, R. R. and Kautz, S. A. (2003). Biomechanics and muscle coordination of human walking. Part II: Lessons from dynamical simulations and clinical implications. *Gait Posture* **17**, 1-17.